

High Power and High Linearity Traveling wave Electroabsorption Modulator

P. K. L. Yu*, W. S. C. Chang, G. Li, I. Shubin, Y. Zhuang, J.X. Chen, Y.Wu,
Dept. of ECE, Jacobs School, University of California, San Diego, La Jolla, CA 92093

M. J. Hayduk, R. J. Bussjager

Air Force Research Laboratory, Sensors Directorate, 25 Electronic Pkwy, Rome, NY 13441

ABSTRACT

Design for high efficiency, high power traveling wave electroabsorption modulator using Intra-Step-Barrier Quantum Well (IQW) and Peripheral Coupled waveguide (PCW) designs are presented. Both of these designs have separately yielded EAMs with high optical power handling and low V_{π} properties, in an analog fiber link configuration. The IQW EAM has low V_{π} (~0.73 V) and high power handling (100 mW). The lumped element IQW EAM has achieved a link gain of -16 dB, a multi-octave SFDR of 110 dB-Hz^{2/3} and a single-octave SFDR of 121dB-Hz^{4/5} at the 1543 nm wavelength. The PCW MQW EAM with lumped element configuration can achieve a low link loss, a high multi-octave SFDR at the same wavelength. The traveling wave properties of these EAMs are under investigation.

Keywords: Electroabsorption modulator, analog fiber link, large dynamic range, high saturation power

INTRODUCTION

Fiber-optic communication takes advantage of characteristics of light and fibers to transmit information, using formats such as intensity, phase, frequency and polarization modulation. Among these, the intensity modulation is presently the most popular for optical fiber communication systems, mainly due to the simplicity of envelope detection. The performance requirements for optical modulations are different between analog systems and digital systems. For instance, the analog systems commonly use small-signal modulation, with primary requirements such as large incremental slope efficiency, wide bandwidth, high linearity and low noise, etc. Digital systems commonly use on/off keying modulation format, with primary requirements such as large on/off extinction ratio, high data rate (i.e., wide bandwidth), low or controlled chirp, large signal to noise ratio, etc. Nevertheless, both analog and digital systems share some common grounds such as high optical power handling capability, small optical loss, polarization insensitivity, and stable performance over ambient temperature variation and time.

A common fiber-optic link consists of three principal parts. At the input is a modulator, which imposes the RF signal onto an optical carrier. The modulated output is coupled to an optical fiber and detected by a photodetector, where it is demodulated back into an RF signal. One of the important figures of merit for any analog fiber-optic link is its conversion efficiency (or RF link gain). The link gain of an intrinsic externally modulated link is proportional to the square of the product of the optical power, the optical insertion efficiency, and the slope efficiency of the modulator [1]. Previously, a high RF link gain (>30 dB) externally modulated link has been experimentally demonstrated at 150 MHz using a LiNbO₃ Mach-Zehnder modulator [2].

For externally modulated links, a high speed electroabsorption modulator (EAM) with high saturation optical power is very desirable due to its small size. EAMs using multiple-quantum-well (MQW) active layers have been

* Phone: 858-534-6180, Fax : 858-534-0556, Email : yu@ece.ucsd.edu

popular as they typically possess a large absorption-coefficient change with applied electric field. However, common MQW modulator structures have shown relatively small saturation optical power primarily due to the field-screening effect from the trapped photogenerated carriers inside the well [3]. EAMs with improved saturation properties have been demonstrated using lower barrier heights by applying appropriate strain at the well/barrier interface [4].

In our work, we propose two alternate novel approaches to enhance the optical power handling: (1) A material engineering approach to enhance the saturation power via the use of a barrier step inside the well to suppress the onset of the (red shift) quantum-confined Stark effect to a higher electric field [5], (2) A waveguide approach to enhance the saturation optical power. By delaying the red shift with the intra-step-barrier quantum wells (IQWs), the biasing electric field for the EAM can be increased without reducing the modulation efficiency while the screening effect due to the photogenerated carriers is reduced at higher electric field.

We first report the design and results of the high power electroabsorption modulator employing the IQW for high speed and high power operation with diluted waveguide design to improve the optical coupling.

It should be noted that, despite the broad bandwidth property of the traveling wave (TW) design, prior TW-EAMs are limited in efficiency due to the high propagation loss in the conventional optical waveguide that limits the waveguide to ~ 0.2 mm long. Recently, the Peripheral Coupled Waveguide (PCW) EAM has been demonstrated at UCSD [6,7]. In this approach, the microwave transmission line, as well as the electroabsorption region, is placed at the peripheral, evanescent field region of the optical waveguide mode. In this way the design of the microwave waveguide can be separated from that of the optical waveguide. The microwave waveguide can be designed with the appropriate dimensions that yield the desirable impedance, phase velocity and microwave attenuation. The optical waveguide can support a large mode size that matches to that of the single mode fiber. It can have a small residual attenuation and a low optical confinement factor that ensures a high optical saturation power.

INTRA-STEP-BARRIER QUANTUM WELL

The basic operation of the IQW is depicted in Figs. 1 (a)-(d) which show the schematic band diagrams of the InGaAsP/InGaAs IQW with an InGaAs ($E_g = 0.75$ eV) well, InGaAsP barriers ($E_g = 1.08$ eV), and an InGaAsP ($E_g = 0.77$ to 0.89 eV) intra-step-barrier lattice-matched to InP, and with increasing electric field (Fig. 1 b to d). Also shown are the energy levels and the envelope wave functions associated with the conduction band and the heavy hole sub-band [5].

At zero electric field, Fig. 1a shows that the heavy hole is more tightly confined in the well than the electron. This is mainly due to the large effective-mass difference between the electron and the heavy hole. As the electric field is increased, the electron energy level decreases in a manner typical of the Stark shift. On the other hand, the hole energy level increases initially to overcome the intra-step-barrier. This effectively suppresses the red shift in the transition energy. As the hole becomes more confined in the region of the intra-step-barrier, the hole energy level starts to decrease and the overall transition energy then undergoes red shift. Two main results are observed from IQWs: the biasing electric field for maximum slope efficiency is much higher than the that of the conventional quantum well; a sharper transition as the hole is raised across the barrier step, leading to a higher modulator slope efficiency.

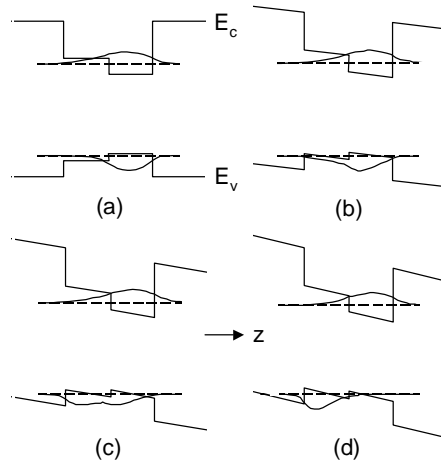


Fig.1. InGaAsP/InGaAs IQW at increasing electric field with the conduction band and heavy hole sub-band energy levels and the corresponding envelope wave functions [5].

For instance, for a 15-period intra-step quantum wells incorporated in the intrinsic layer, with the barrier, intra-step-barrier, and well layers having thickness of 7, 6 and 5 nm respectively, we numerically solve the Schrödinger's equation using the effective mass and the envelope function approximations. From the simulation, we estimate a zero-field exciton transition wavelength of 1465 nm between the first heavy hole subband and the first conduction subband. Its variation with the applied field is shown in Fig. 2.

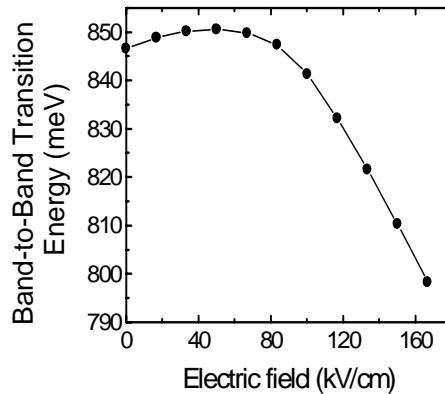


Fig. 2. Transition energy between first heavy hole subband to first conduction subband as a function of the electric field.

PERIPHERAL COUPLED WAVEGUIDE

High RF link gain requires high saturation power, low insertion loss and low equivalent V_π for an EAM. PCW-EAM can easily have much larger optical saturation power than a conventional waveguide EAM due to its small confinement factor in the EA layer. A conventional TW-EAM waveguide normally has a confinement factor of 20 ~ 30%, while our PCW-EAM can have a confinement factor as low as 2~5%. Optical saturation caused by the

screening effect of the generated photo carriers in the EA layer can thus be much reduced. Fig. 3 shows a simulated mode profile of the PCW-EAM.

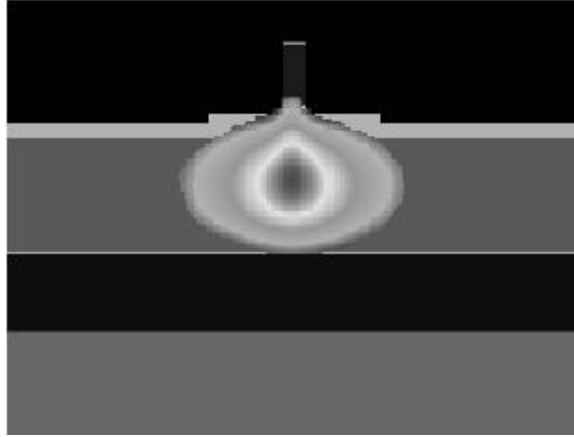


Fig. 3. PCW mode pattern, the EA region is located in the narrow top ridge, the mode is highest in intensity in the lower waveguiding region.

In the PCW-EAM, the insertion loss can be decreased by reducing the waveguide propagation loss and by improving the coupling to the fiber. The large waveguide mode submerged underneath the narrow ridge shown in Fig. 3 encounters a small surface scattering loss and a small residual loss since the waveguiding layer has higher bandgap energy than the photon energy. Experimentally we have measured residual optical propagation loss as low as ~ 2 dB/mm. The large optical mode eases the coupling to single mode fiber (SMF). Simulation shows that the coupling coefficient from/to a lensed fiber can be as high as 95%, and around 70% from/to a cleaved SMF. These are critical for getting a small insertion loss.

For EAM link the RF link gain is proportional to the square of the product of incident power, optical insertion loss and normalized slope efficiency at the bias point. In term of the normalized slope efficiency, a parameter called “Equivalent V_π ” can be defined as:

$$(V_\pi)_{\min} = \frac{\pi}{2 \left. \frac{dT_N}{dV} \right|_{\max}} \propto d_i \frac{\alpha}{\alpha'} \Big|_{\text{bias}} \quad (1)$$

where α and α' the absorption coefficient and its derivative with respect to electric field; α_{bias} is the absorption coefficient at DC bias; d_i is the thickness of the undoped electroabsorption region. Eq. 1 implies that by reducing d_i and increasing α/α' one can obtain a low V_π . By incorporating the peripheral coupled waveguide and the IQW in the TW EAM structure, we can a large obtain α/α' and small d_i thus resulting in a wide bandwidth and highly efficient intensity modulator.

PERFORMANCE OF AN IQW EAM

An InGaAsP/InGaAs IQW EAM with 15 wells and 1.2 μm thick lower waveguiding layer was designed and fabricated. The materials structure is grown using MOCVD. The IQWs were designed for operation at 1550 nm wavelength. For this structure, we have measured an optical propagation loss of 4 dB/mm at a wavelength of 1568 nm. Fig. 4 summarizes the transfer curve of 1.1 mm long device with bare facets, as a function of laser wavelength.

The input light is TE polarized and at 1 mW. From Fig. 4 we extract the optical insertion (without AR coating) and the equivalent V_{π} at these wavelengths; they are summarized in Table 1.

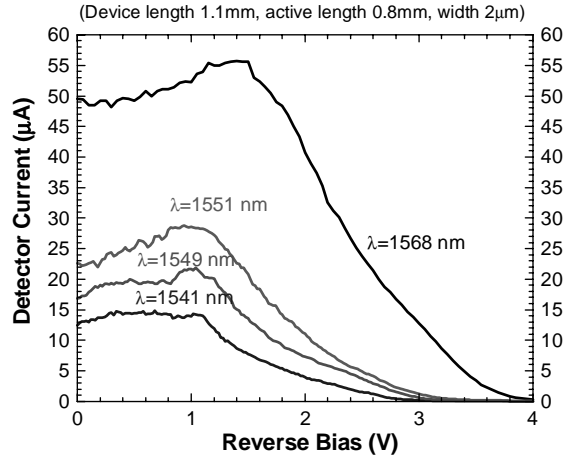


Fig. 4. Transfer curve characteristics of a 1.1 mm long IQW-PCW as various wavelengths [7].

The measured RF link gain can be improved further by optimizing the waveguide layer (i.e., making it thicker) and by modifying the IQW layer thickness and the number of periods. Fig. 5 shows the results of the link gain measurement up to 100 mW at 1 GHz for a 0.35 mm long device at detuned wavelength $\lambda = 1568$ nm as a function of optical power. The detector responsivity is 0.7 A/W.

Table 1. V_{π} and the optical insertion loss at various wavelengths.

| Wavelength h | V_{π} (V) | Insertion loss | V_{bias} (V) |
|-----------------|------------------|-------------------|--------------------------|
| 1541 nm | 0.8 | 16.7 dB | 1.2 |
| 1549 nm | 0.7 3 | 15 dB | 1.4 |
| 1551 nm | 0.8 3 | 13.8 dB | 1.5 |
| 1568 nm | 1.9 | 10.3 dB | 1.6 |

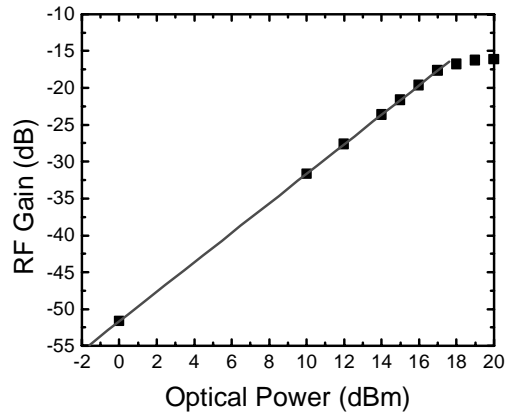


Fig. 5. Measured RF link gain of the IQW-EAM that is 0.35 mm long, at 1543 nm wavelength.

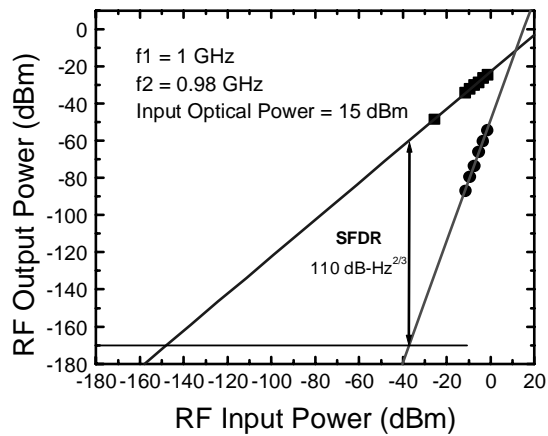


Fig. 6. Two-tone multi-octave SFDR measurement for a 0.35 mm long device with lumped element electrode. The device is biased at the 2nd order null point.

A two-tone spurious free dynamic range (SFDR) measurement is done for a 0.35 mm long device with a lumped element electrode at a frequency of ~600 MHz. The results are depicted in Fig. 6, a multi-octave SFDR of 110 dB-Hz^{2/3} and input third order intercept (IIP3) of ~ 15 dBm is observed at an input optical power of 15 dBm and at 1543 nm wavelength.

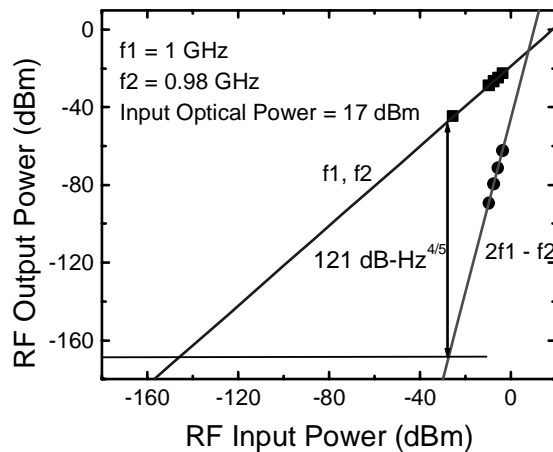


Fig. 7. Single octave SFDR measurement of the same device at the 3rd order null point.

We have also performed the single octave SFDR of the device. The optical input power to the EAM is 50 mW and the bias voltage is 3.3 V. The two RF tones are at 1 GHz and 0.98 GHz, respectively. From the insertion loss at bias point and the input optical power, we estimate that the shot-noise-dominated noise floor is -168 dBm. The two-tone single-octave SFDR is $121\text{dB-Hz}^{4/5}$, as shown in Fig. 7.

LOW LOSS MQW EAM USING PCW

As mentioned previously, by introducing the peripheral coupled waveguide (PCW) structure into the EAM, we can decouple the microwave electrode design and the optical design. The microwave electrode, including the EA region, is placed only peripheral to the optical waveguide mode, in its evanescent field. The low confinement factor in the EA layer reduces the photo-generated current per unit length, and thus enhances the optical power handling of the EAM. The design of the microwave electrode will minimally affect the optical mode, so one can use a very small EA layer thickness to lower the V_π . As the guided optical mode is located away from the surface, it encounters a much smaller propagation loss. Thus the insertion loss is reduced significantly. This allows us to increase the device length to ensure a low V_π . Furthermore, the optical waveguide will have a large mode size to match to the single-mode fiber mode.

To demonstrate this concept, a PCW EAM with a lumped- electrode is reported in this paper, in which high optical saturation, low insertion loss and low V_π all work together to give us a low RF link insertion with large spurious-free dynamic range.

The p-i(MQW)-n waveguide modulator is grown on a semi-insulating InP substrate. The active EA region ($0.1\ \mu\text{m}$ thick) consists of five periods of InGaAsP wells and InGaAsP barriers. The exciton absorption peak of this MQW is set at 1480 nm. Underneath the active layer is a $1.7\ \mu\text{m}$ thick InGaAsP (1.11eV bandgap) lower cladding layer which leads to an optical waveguide structure like that of one-sided large optical cavity where the majority of the optical mode is confined in this lower cladding layer. The RF link gain of an externally modulated optical link using this EAM was measured at 500 MHz at different optical input power levels. The modulator is biased at the second order null point. The RF link gain versus optical input power exhibits a slope of 2 in a log-log plot, as shown in Fig. 8. At up to 80 mW optical power, the modulator did not show any sign of saturation. A link gain of $-3\ \text{dB}$ was obtained at 80 mW input power.

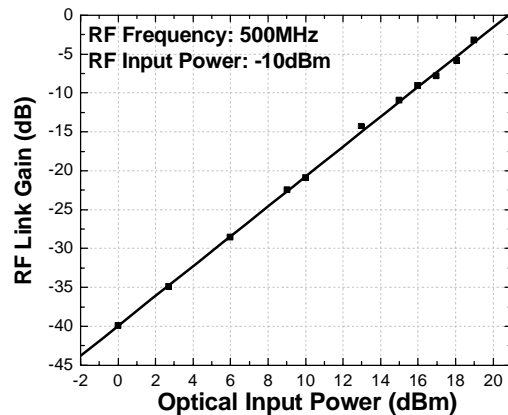


Fig. 8. RF link gain versus input optical power of the PCW-EAM.

The single octave and the multi-octave SFDR of the PCW EAM and the design for the traveling wave electrode are on-going and will be presented at the meeting.

CONCLUSION

In summary, we have successfully demonstrated a diluted waveguide IQW EAM structure that has low V_{π} (~ 0.73 V) and high power handling (100 mW). The lumped element IQW EAM has achieved a link gain of -16 dB, a multi-octave SFDR of $110 \text{ dB-Hz}^{2/3}$ and a single-octave SFDR of $121 \text{ dB-Hz}^{4/5}$ at the 1543 nm wavelength.

We have demonstrated a highly efficient peripheral coupled waveguide electroabsorption modulator for an externally modulated analog fiber-optic link. The PCW EAM is demonstrated to have very high saturation power with low RF insertion loss.

ACKNOWLEDGMENT

This work at the University of California, San Diego is partially sponsored by AFRL, NSF ANIR, DARPA RFLICS Program and CCAT.

REFERENCES

- [1] C. Cox III, G.E. Betts, L.M. Johnson, "An analytic and experimental comparison of direct and external modulation in analog fiber-optic links", *IEEE Trans. Microwave Theory Tech.*, vol. 38., no.5, pp.501-9, 1990.
- [2] C. Cox III, E. Ackerman, G. Betts, "Relationship between gain and noise figure of an optical analog link", *1996 IEEE MTT-S International Microwave Sympo. Digest*, vol.3, pp.1551-4, 1996.
- [3] T. H. Wood, J. Z. Pastalan, C. A. Burrus. Jr., B. C. Johnson, B. I. Miller, J. L. deMiguel, U. Koren, and M. G. Young, *Appl. Phys. Lett.* 57, 1081 (1990).
- [4] R. Sahara, K. Morito, K. Sato, Y. Kotaki, H. Soda, and N. Okazaki, *Photon. Technol. Lett.* 7, 1004 (1995).
- [5] D. S. Shin, P. K. L. Yu, and S. A. Pappert, *J. Appl. Phys.* 89, 1515 (2001).
- [6] P.K.L. Yu, W.S.C. Chang, Y. Zhuang, G.L. Li, "Advances in Traveling-wave Electroabsorption Modulators for Analog Applications", *Proc. of the LEOS'01*, vol. 2, pp.540-541, 2001.
- [7] Y. Zhuang, Y. Wu, W. S. C. Chang, P. K. L. Yu, S. Mathai, M. Wu, D.Tishinin, K. Y. Liou, presented at *IEEE, IMS 2003*, Philadelphia, June 2003.